Effect of uncoordinated network interference on UWB autocorrelation receiver

Effect of Uncoordinated Network Interference on UWB Autocorrelation Receiver

Alberto Rabbachin*, Tony Q. S. Quek†, Ian Oppermann‡, and Moe Z. Win§
*Institute for the Protection and Security of the Citizens, European Commission, JRC, 21027 Ispra, Italy
†Institute for Infocomm Research, 1 Fusionopolis Way, #21-01 Connexis South Tower, Singapore 138632
‡Centre for Wireless Communications, University of Oulu, P.O.Box 4500, 90014-Oulu, Finland
§Massachusetts Institute of Technology, Cambridge, MA 02139, USA

***Abstract*—Over the last few years there has been an emerging interest in ultrawideband (UWB) communications in wireless sensor networks, mainly due to their low-complexity and low-power consumption. In particular, auto-correlation receiver (AcR) is a potential candidate for such applications. However, the presence of network interference, especially interference between uncoordinated UWB networks, will severely degrade the performance of such receiver. In this paper, we analyze the bit error probability performance of the AcR in the presence of UWB interference. We model the network interference as an aggregate UWB interference, generated by elements of uncoordinated UWB networks scattered according to a spatial Poisson process. Our analytical framework allows a tractable performance analysis and still provides sufficient insight into the effect of uncoordinated network interference on UWB systems.**

I. Introduction

There has been an increasing interest in ultrawideband (UWB) technology, particularly as a strong candidate for low-power consumption sensor network applications [1], [2]. In particular, auto-correlation receiver (AcR) has been considered as a potential low-complexity and low-sampling rate solution in the IEEE 802.15.4a standardization process [3]. The wide spreading of sensor networks using UWB communications to ensure wireless connectivity will inevitably lead to increasing network interference (NWI), especially between uncoordinated networks.

Since the main NWI is likely to be contributed by a few dominant interferers at close range, the UWB NWI tends to be heavy-tailed distributed. Moreover, with the low duty-cycle of UWB transmissions, the interference behaves in an impulsive behavior. This complicates the modeling of UWB NWI since we can no longer use the Gaussian approximation [4]–[6]. In [4]–[6], the authors do not consider or only partially consider the spatial distribution of the interferers and the propagation effects of the interfering signals. Furthermore, the studies of non-coherent receiver structures are missing in these literatures.

In modeling impulsive signals, the stable distribution provides a valuable mathematical tool, which has been proven to be useful for modeling a wide class of impulsive noise processes [7], [8]. In the case of NWI, it is also necessary to account for the stochastic geometry of the interfering sources to obtain a more accurate statistical model of the network interference. By assuming a Poisson field of interferers, several works have analyzed the effect of narrowband interference on narrowband [7]–[9] and UWB systems [10], respectively. However, to the best of our knowledge, there is hardly any results available that analyze the effect of uncoordinated UWB NWI, particularly, when non-coherent receiver structures are employed.

In this paper, we analyze the bit error probability (BEP) performance of the AcR in the presence of uncoordinated UWB NWI. We show that multivariate stable random variables (r.v's) can be used to describe the statistics of the NWI. The proposed model for the aggregate interference accounts for the spatial distribution of the UWB interferers and the propagation characteristics of the interference signals.

The paper is organized as follows: Section II presents the signaling schemes, the channel model, and the receiver structure. Section III describes the statistical characterization of the UWB interference. The BEP analysis of AcR in the presence of UWB NWI is given in Section IV. Numerical results and conclusion are provided in Section V and VI, respectively.

II. System and channel models

The transmitted signal for user k can be decomposed into a reference signal $b_{\rm r}^{(k)}(t)$ and a data modulated signal $b_{\rm d}^{(k)}(t)$ as follows:

$$s^{(k)}(t) = \sum_i b_{\rm r}^{(k)}(t - iT_{\rm s}) + d_i^{(k)} b_{\rm d}^{(k)}(t - iT_{\rm s}), \qquad (1)$$

where $d_i^{(k)} \in \{-1, 1\}$ is the ith data symbol and $T_{\rm s} = N_{\rm s} T_{\rm f}^{\rm TR}$ is the symbol duration, such that $N_{\rm s}$ and $T_{\rm f}^{\rm TR}$ are the number of pulses per symbol and the average pulse repetition period, respectively [2]. The reference and data modulated signals are given by

$$b_{\rm r}^{(k)}(t) = \sum_{j=0}^{\frac{N_{\rm s}}{2}-1} \sqrt{E_{\rm p}^{\rm TR}} a_j^{(k)} p(t - j2T_{\rm f}^{\rm TR} - c_j^{(k)} T_{\rm p}),$$

$$b_{\rm d}^{(k)}(t) = \sum_{j=0}^{\frac{N_{\rm s}}{2}-1} \sqrt{E_{\rm p}^{\rm TR}} a_j^{(k)} p(t - j2T_{\rm f}^{\rm TR} - c_j^{(k)} T_{\rm p} - T_{\rm r}),$$

where $b_{\rm d}^{(k)}(t)$ is equal to a version of $b_{\rm r}^{(k)}(t)$ delayed by $T_{\rm r}$. In TH signaling, $\{c_j^{(k)}\}$ is the pseudo-random sequence of the

9781-4244-2931-8/09/$25.00 ©2009 IEEE

kth user, where $c_j^{(k)}$ is an integer in the range $0 \leq c_j^{(k)} < N_\mathrm{h}$ and N_h is the maximum allowable integer shift. The bipolar random amplitude sequence $\{a_j^{(k)}\}$ together with TH sequence are used to mitigate interference and to support multiple access. The term $p(t)$ is a unit energy bandpass pulse with duration T_p and center frequency f_c. The energy of the transmitted pulse is $E_\mathrm{p}^\mathrm{TR} = E_\mathrm{s}^\mathrm{TR}/N_\mathrm{s}$ where E_s^TR is the symbol energy associated with TR signaling.[1] The duration of the received UWB pulse is $T_\mathrm{g} = T_\mathrm{p} + T_\mathrm{d}$, where T_d is the maximum excess delay of the channel. We consider $T_\mathrm{r} \geq T_\mathrm{g}$ and $(N_\mathrm{h} - 1)T_\mathrm{p} + T_\mathrm{r} + T_\mathrm{g} \leq 2T_\mathrm{f}^\mathrm{TR}$, where T_r is the time separation between each pair of data and reference pulses to preclude intra-symbol interference (isi) and inter-symbol interference (ISI).

The received signal can be expressed as $r(t) = h(t) * s(t) + n(t)$, where $h(t)$ is the impulse response of the channel given by

$$h(t) = \sum_{l=1}^{L} h_l \delta(t - \tau_l), \tag{3}$$

where h_l and τ_l are the attenuation and the delay of the lth path component, respectively. The term $n(t)$ is zero-mean, white Gaussian noise with two-sided power spectral density $N_0/2$. As in [11], we consider a resolvable dense multipath channel, i.e., $|\tau_l - \tau_j| \geq T_\mathrm{p}, \forall l \neq j$, where $\tau_l = \tau_1 + (l-1)T_\mathrm{p}$ and $\{h_l\}_{l=1}^{L}$ are statistically independent r.v.'s. We can express $h_l = |h_l| \exp(j\phi_l)$, where $\phi_l = 0$ or π with equal probability. The AcR first passes the received signal through an ideal bandpass zonal filter (BPZF) with center frequency f_c to eliminate out-of-band noise [2]. If the bandwidth W of the BPZF is large enough, then the signal spectrum will pass through the filter undistorted. In the rest of the paper, we focus on a single user system and we will suppress the index k for notational simplicity. In this case, following the channel model described above, the output of the BPZF can be written as[2]

$$\begin{aligned} &\widetilde{r}_\mathrm{TR}(t) \\ &= \sum_i \sum_{l=1}^{L} \left[h_l b_\mathrm{r}(t - iT_\mathrm{s} - \tau_l) + h_l d_i b_\mathrm{d}(t - iT_\mathrm{s} - \tau_l)\right] + \widetilde{n}(t), \end{aligned} \tag{4}$$

where $\widetilde{n}(t)$ represents the noise process after the BPFZ and the output of the AcR can be written as

$$Z_\mathrm{TR} = \sum_{j=0}^{\frac{N_\mathrm{s}}{2}-1} \int_{j2T_\mathrm{f}^\mathrm{TR}+T_\mathrm{r}+c_jT_\mathrm{p}}^{j2T_\mathrm{f}^\mathrm{TR}+T_\mathrm{r}+c_jT_\mathrm{p}+T} \widetilde{r}_\mathrm{TR}(t)\, \widetilde{r}_\mathrm{TR}(t - T_\mathrm{r}) dt, \tag{5}$$

where the integration interval T determines the number of multipath components (or equivalently, the amount of energy) as well as the amount of noise captured by the receiver.[3]

III. UWB INTERFERENCE

A. Multiple UWB interferers

We model the spatial distribution of the multiple UWB interferers according to a homogeneous Poisson point process in a two-dimensional plane [9]. The probability that k nodes lie inside region $\mathcal{R}$ depends only on the area $A_\mathcal{R} = |\mathcal{R}|$, and is given by [12]

$$\mathbb{P}\{k \in \mathcal{R}\} = \frac{(\lambda A_\mathcal{R})^k}{k!} e^{-\lambda A_\mathcal{R}}, \tag{6}$$

where λ is the spatial density (in nodes per unit area).

Using our system model in Section II, the transmitted signal from the nth UWB interferer is given by

$$I^{(n)}(t) = \sqrt{P^\mathrm{I}} \sum_i b_i^{(n)} \left(t - iN_\mathrm{s}^\mathrm{I} T_\mathrm{f}^\mathrm{I}\right), \tag{7}$$

where $b_i^{(n)}(t) \triangleq \sum_{j=1}^{\frac{N_\mathrm{s}}{2}} e_i^{(n)} a_j^{(n)} p(t - jT_\mathrm{f} - c_j^{(n)} T_\mathrm{p} - d_i^{(n)} \Delta^\mathrm{I})$, $P^\mathrm{I} \triangleq E_\mathrm{b}^\mathrm{I}/T_\mathrm{f}^\mathrm{I} N_\mathrm{s}^\mathrm{I}$ is the average power at the border of the near-field zone of each interfering transmitter antenna, and T_f^I is the pulse repetition period average, such that it is assumed to be the same for all UWB interferers and all interferer signals also have the same symbol duration $T_\mathrm{s}^\mathrm{I} = T_\mathrm{f}^\mathrm{I} N_\mathrm{s}^\mathrm{I}$.[4] Note that we intentionally write (7) to account for two possible modulations, namely binary pulse amplitude modulation (BPAM) and binary pulse position modulation (BPPM). The term $e_i^{(n)} \in \{-1, 1\}$ is the ith data symbol for BPAM modulation, $d_i^{(n)} \in \{0, 1\}$ is the ith data symbol for BPPM modulation, and Δ^I is the position modulation shift. The jth element of the random hopping and amplitude sequences are denoted by $\{c_j^{(n)}\}$ and $\{a_j^{(n)}\}$, where $0 < c_j^{(n)} < N_\mathrm{h}^\mathrm{I}$, N_h^I is the maximum shift associated with the hopping code, and $a_j^{(n)} \in \{-1, +1\}$ for all j and n. The average pulse repetition interval is considered long enough such that isi and ISI can be ignored. For notational convenience, we define $\Psi^{(n)} \triangleq \left\{\{e_i^{(n)}\}, \{c_j^{(n)}\}, \{a_j^{(n)}\}, \{h_l^{(n)}\}\right\}$.

Using the spatial model in (6), the aggregate UWB interference signals received at the output of the BPZF of the desired user is given by

$$\zeta(t) = \sum_{n=1}^{\infty} \zeta^{(n)}(t), \tag{8}$$

and $\zeta^{(n)}(t)$ denotes the signal from the nth UWB interferer and it can be expressed as

$$\zeta^{(n)}(t) = \frac{e^{\sigma_\mathrm{I} G^{(n)}}}{\left(R^{(n)}\right)^\nu} \sqrt{P^\mathrm{I}} v^{(n)} \left(t - D^{(n)}\right), \tag{9}$$

where the shadowing term $e^{\sigma_\mathrm{I} G^{(n)}}$ follows a log-normal distribution with shadowing parameter σ_I and $G^{(n)} \backsim \mathcal{N}(0, 1)$.[5] According to the far-field assumption, the signal power decays as $1/(R^{(n)})^{2\nu}$, where $R^{(n)}$ is the distance between the nth UWB interferer and the desired user and ν is the amplitude loss exponent. To model time-asynchronism of the UWB interfering signals, we define $D^{(n)}$ as a uniformly distributed r.v. and $v^{(n)}(t)$ in (9) can be further expressed as

$$v^{(n)}(t) = \sum_i b_i^{(n)}(t - iN_\mathrm{s}^\mathrm{I} T_\mathrm{f}^\mathrm{I}) * h^{(n)}(t - iN_\mathrm{s}^\mathrm{I} T_\mathrm{f}^\mathrm{I}), \tag{10}$$

[1] Note that the transmitted energy is equally allocated among $N_\mathrm{s}/2$ reference pulses and $N_\mathrm{s}/2$ modulated pulses.

[2] Note that we assume perfect symbol synchronization at the receiver.

[3] Note that the optimal integration interval depends on the shape of the power delay profile and signal-to-noise ratio (SNR).

[4] Furthermore, we assume that all UWB interferers use the same pulse waveform as the desired signal and their signals are undistorted at the output of the BPZF.

[5] We use $\mathcal{N}(0, \sigma^2)$ to denote a Gaussian distribution with zero-mean and variance σ^2.

where $h^{(n)}(t) = \sum_{l=0}^{L-1} |h_l^{(n)}| e^{-j\phi_l^{(n)}} \delta(t - \tau_l^{(n)})$ is the channel impulse response of the nth UWB interferer-receiver link.[6]

B. AcR

Conditioning on $\{\Psi^{(n)}\}$, $\{c_j\}$, $\{a_j\}$, and $\{h_l\}$, it can be shown that the probability of $Z_{\text{TR}} < 0$ for $d_0 = +1$ can be expressed as [13]

$$\mathbb{P}\{Y_{\text{TR},1} - Y_{\text{TR},2} < 0\} = \frac{1}{2} + \frac{1}{\pi} \int_0^\infty \left(\frac{1}{1+v^2}\right)^q \mathfrak{Re}\left\{\frac{\exp\left(\frac{-jv\mu_{Y_{\text{TR},1}}}{1+jv} + \frac{jv\mu_{Y_{\text{TR},2}}}{1-jv}\right)}{jv}\right\} dv. \quad (11)$$

where $Y_{\text{TR},1}$ and $Y_{\text{TR},2}$ are two non-central chi-square distributed random variable. Using the sampling expansion the non centrality parameters of $Y_{\text{TR},1}$ and $Y_{\text{TR},2}$ can be written as

$$\begin{aligned}\mu_{Y_{\text{TR},1}}^{(\text{UWB})} &\triangleq \frac{2}{N_0} \sum_{j=0}^{\frac{N_s}{2}-1} \sum_{m=1}^{2WT} \frac{1}{2W} \left[w_{j,m} + \frac{\zeta_{1,j,m} + \zeta_{2,j,m}}{2}\right]^2, \\ &= \underbrace{\frac{E_s^{\text{TR}}}{N_0} \sum_{l=1}^{L_{\text{CAP}}} h_l^2}_{\triangleq \mu_{\text{A,TR}}} + \underbrace{\sum_{j=0}^{\frac{N_s}{2}-1} \sum_{m=0}^{2WT} \frac{1}{2N_0} \frac{r_{1,j,m}^2}{2W}}_{\triangleq \mu_{\text{B,TR}}^{(\text{UWB})}} \\ &+ \underbrace{\sum_{j=0}^{\frac{N_s}{2}-1} \sum_{m=1}^{2WT} \frac{1}{2N_0} \frac{r_{1,j,m} w_{j,m}}{2W}}_{\triangleq \mu_{\text{C,TR}}^{(\text{UWB})}}, \end{aligned} \quad (12)$$

$$\begin{aligned}\mu_{Y_{\text{TR},2}}^{(\text{UWB})} &\triangleq \frac{2}{N_0} \sum_{j=0}^{\frac{N_s}{2}-1} \sum_{m=0}^{2WT} \frac{1}{2W} \left[\frac{\zeta_{2,j,m} - \zeta_{1,j,m}}{2}\right]^2 \\ &= \sum_{j=0}^{\frac{N_s}{2}-1} \sum_{m=1}^{2WT} \frac{1}{2N_0} \frac{r_{2,j,m}^2}{2W}, \end{aligned} \quad (13)$$

where $w_{j,m}$, $\zeta_{1,j,m}$ and $\zeta_{2,j,m}$, for odd m (even m), are the real (imaginary) parts of the samples of the equivalent low-pass version of $w_j(t)$, $\zeta_{1,j}(t) \triangleq \zeta(t + jT_f + c_jT_p)$ and $\zeta_{2,j}(t) \triangleq \zeta(t + jT_f + c_jT_p + T_r)]$ respectively, sampled at Nyquist rate W over the interval $[0, T]$. where $r_{1,j,m} \triangleq \zeta_{1,j,m} + \zeta_{2,j,m}$ and $r_{2,j,m} \triangleq \zeta_{2,j,m} - \zeta_{1,j,m}$. From (12) to (13), it can be observed that we still need to derive some statistical model for the aggregate UWB interference. In the following, we define the complex vector $\bar{\boldsymbol{\zeta}}_{1,j}$ which composed of WT samples of $\zeta(t)$ defined in (8). Specifically, the vector $\bar{\boldsymbol{\zeta}}_{1,j}$ can be written as

$$\bar{\boldsymbol{\zeta}}_{1,j} = \sum_{n=1}^{\infty} \frac{e^{\sigma_I G^{(n)}}}{\left(R^{(n)}\right)^{\nu}} \bar{\mathbf{v}}_{1,j}^{(n)}, \quad (14)$$

where $\bar{\mathbf{v}}_{1,j}^{(n)}$ is the vector of complex samples of the equivalent low-pass version of $v^{(n)}(t + c_jT_p + jT_f - D^{(n)})$, such that $\mathbf{v}_{1,j,m}^{(n)}$ at the sampling instant m are a sequence of i.i.d. r.v's in n. If the signal of the nth UWB interferer is present in the sampling instant m, each sample can be written as

$$\mathbf{v}_{1,j,m}^{(n)} = p\left(\tau^{(n)}\right) h_m^{(n)} \sqrt{\exp(-\epsilon^{\text{I}}(m - T^{(n)}))} \Theta_m^{(n)}, \quad (15)$$

where $\tau^{(n)} \triangleq (D^{(n)} \bmod T_p)$ is a r.v. uniformly distributed over $[0, T_p)$, $T^{(n)}$ is a discrete r.v. uniformly distributed over $[0, 1, \ldots, L-1]$, $h_m^{(n)}$ is a r.v. with variance $1/\sum_{l=1}^{L} \exp(-\epsilon^{\text{I}}(l))$ and distributed according to the small-scale fading, and $\Theta_m^{(n)} = \cos(\phi_m^{(n)}) - \jmath \sin(\phi_m^{(n)})$ with $\phi_m^{(n)}$ uniformly distributed over $[0, 2\pi)$.[7] Considering that the complex r.v. $\Theta_m^{(n)}$ is circularly symmetric (CS), as for the case in the presence of narrowband interference [10], $\boldsymbol{\zeta}_{1,j,m}$ can be described by a stable complex distribution as follows[8]

$$\boldsymbol{\zeta}_{1,j,m} \backsim S_c\left(\frac{2}{\nu}, 0, \gamma_{\text{UWB}}\right), \quad (16)$$

where $\boldsymbol{\zeta}_{1,j,m}$ is the mth complex sample of $\bar{\boldsymbol{\zeta}}_{1,j}$ in (14) and $\gamma_{\text{UWB}} \triangleq \lambda\pi C_{2/\nu}^{-1} e^{2\sigma_I^2/\nu^2} \mathbb{E}\{|\mathfrak{Re}\{\mathbf{v}_{1,j,m}\}|^{2/\nu}\}$, such that $\mathbb{E}\{|\mathfrak{Re}\{\mathbf{v}_{1,j,m}\}|^{2/\nu}\} = \frac{T_g^I}{T_f^I} MFP$ and the associated parameters M, F, P are, respectively, given by

$$\begin{aligned} M &= \mathbb{E}\left\{|h_m^{(n)}|^{2/\nu}\right\} \mathbb{E}\left\{\left(\sqrt{\exp(-\epsilon T^{(n)})}\right)^{2/\nu}\right\} \\ F &= \mathbb{E}_n\{|e_i^{(n)} a_j^{(n)}|^{2/\nu}\}, \\ P &= \mathbb{E}\{|p\left(\tau^{(n)}\right)|^{2/\nu}\} \mathbb{E}\left\{|\cos(\phi_m)|^{2/\nu}\right\}. \end{aligned}$$

Note that the components of the aggregate interference vector $\bar{\boldsymbol{\zeta}}_{1,j}$ in (14) are identically distributed but mutually dependent [15].[9] To make our analysis tractable, we assume that the $S\alpha S$ vector $\bar{\boldsymbol{\zeta}}_{1,j}$ is spherically symmetric since spherically symmetric vectors have the characteristic of being sub-Gaussian, which implies that they can be decomposed as

$$\bar{\boldsymbol{\zeta}}_{1,j} = \sqrt{V} \bar{\mathbf{G}}_{1,j}, \quad (17)$$

where $V \sim \mathcal{S}(\alpha/2, 1, \cos(\frac{\pi\alpha}{4}))$ and $\bar{\mathbf{G}}_{1,j}$ is a multivariate Gaussian random vector with covariance matrix $\bar{\Sigma}$. Unfortunately, $\bar{\boldsymbol{\zeta}}_{1,j}$ is spherically symmetric only for some scenario. To ensure the spherical symmetry of the resulting aggregate interference vector for more general scenario, we modify each received interference signal as

$$\boldsymbol{v}_{1,j}^{\prime(n)}(t) = z^{(n)} d_\alpha^{-\alpha} \sum_{m=1}^{WT_f^I} \mathbf{G}_{1,j,m} p(t - mT_p), \quad (18)$$

[6] For simplicity, we consider the channels from all UWB interferers have the same maximum excess delay T_g^I.

[7] As suggested in [14], since the low-pass equivalent version of a signal is complex, we considered the phase of each multipath component uniformly distributed over $[0, 2\pi)$.

[8] We use $\mathcal{S}_c(\alpha, \beta, \gamma)$ to denote a CS stable distribution of a complex r.v. with i.i.d. real and imaginary parts, each distributed as $\mathcal{S}(\alpha, \beta, \gamma)$, with characteristic exponent α, skewness β (i.e. $\beta = 0$ in our case), and dispersion γ. For $\alpha \neq 1$ and $\alpha = 1$, the associated CFs are $\psi(jv) = \exp\left[-\gamma|jv|^\alpha \left(1 - j\beta\frac{jv}{|jv|}\tan(\frac{\pi\alpha}{2})\right)\right]$ and $\psi(jv) = \exp\left[-\gamma|jv|\left(1 - j\beta\frac{jv}{|jv|}\ln|jv|\right)\right]$, respectively. Note that in our case the location μ of the real and imaginary r.v.'s is zero [15].

[9] In fact, the aggregate interference vector in (14) is symmetric alpha stable ($S\alpha S$)

where $d_\alpha^\alpha = 2^{\alpha/2}\pi^{-1/2}\left(\Gamma(\frac{\alpha+1}{2})^{-1}\right)$ corresponds to $\mathbb{E}\{|\mathbf{G}_{1,j,m}|^\alpha\}$, $\{\mathbf{G}_{1,j,m}\}_{m=1}^{WT_\mathrm{f}^\mathrm{I}}$ is a sequence of i.i.d complex Gaussian r.v's with zero mean and unit variance, and

$$\mathbb{E}\{|z^{(n)}|^\alpha\} = \frac{T_\mathrm{g}^\mathrm{I}}{T_\mathrm{f}^\mathrm{I}} M \times F \tag{19}$$

Note that each interfering UWB signal now covers the entire frame interval T_f^I and the effect of the duty cycle, channel fading, and channel power delay profile (PDP) are captured in the statistics of $z^{(n)}$, where $z^{(n)} = 0$ with probability $1 - T_\mathrm{g}^\mathrm{I}/T_\mathrm{f}^\mathrm{I}$. The statistics of the aggregate interference obtained by using the interference model in (18) has been shown to be in good agreement with the empirical statistics generated via simulation when realistic conditions are considered.

IV. BEP analysis of the AcR in the presence of multiple UWB interference

A. Type 1 interference

We assume that $T_\mathrm{r} = n_1 T_\mathrm{f}^\mathrm{I}$ and $T_\mathrm{f} = n_2 T_\mathrm{f}^\mathrm{I}$ such that n_1 and n_2 ($n_2 > n_1$) are integers, respectively. For simplicity, we consider no modulation is used and no random amplitude sequences and hopping code sequences are used. Since the interference vector is periodic over each interval T_r for the entire symbol, we have $r_{1,j,m} = 2\sqrt{V}(G_{1,j,m})$ and $r_{2,j,m} = 0$. The non-centrality terms of the r.v.'s $Y_{\mathrm{TR},1}$ and $Y_{\mathrm{TR},2}$ for $d_0 = +1$ can be expressed, respectively, as

$$\mu_{Y_{\mathrm{TR},1}}^{(\mathrm{UWB})} = \underbrace{\frac{E_\mathrm{s}^\mathrm{TR}}{N_0}\sum_{l=1}^{L_\mathrm{CAP}} h_l^2}_{\mu_{\mathrm{A,TR}}} + \underbrace{2\gamma_{\mathrm{UWB}}^{2/\alpha}\frac{P^\mathrm{I} N_\mathrm{s}}{2WN_0} V C_1^{(1)}}_{\mu_{\mathrm{B,TR}}^{(\mathrm{UWB})}} + \underbrace{\sum_{j=0}^{\frac{N_\mathrm{s}}{2}-1}\sum_{m=0}^{2WT}\frac{r_{1,j,m}w_{j,m}}{2WN_0}}_{\mu_{\mathrm{C,TR}}^{(\mathrm{UWB})}}, \tag{20}$$

$$\mu_{Y_{\mathrm{TR},2}}^{(\mathrm{UWB})} = 0, \tag{21}$$

where $C_1^{(1)} = \sum_{m=1}^{2WT} G_{1,j,m}^2$ is a central chi-square distributed r.v. with $2WT$ degrees of freedom. To evaluate the BEP performance, we can use an approximate analytical approach, which assumes $\mu_{\mathrm{C,TR}}^{(\mathrm{UWB})}$ negligible compared to the other first two terms in (20) [13]. In this case, by defining $A^2 \triangleq VC_1^{(1)}$, the conditional BEP can be expressed as

$$P_{e,\mathrm{TR}|A^2} \simeq \frac{1}{2} + \frac{1}{\pi}\int_0^\infty \left(\frac{1}{1+v^2}\right)^{q_\mathrm{TR}} \times \mathfrak{Re}\left\{\frac{\psi_{\mu_\mathrm{TR}}\left(\frac{-jv}{1+jv}\right)\exp\left(\frac{P^\mathrm{I}N_\mathrm{s}}{2WN_0}\frac{-jv}{1+jv}2\gamma_{\mathrm{UWB}}^{\nu}A^2\right)}{jv}\right\} dv. \tag{22}$$

Applying the scaling property, the r.v. A^2 conditioned on $C_1^{(1)}$ has a stable distribution with characteristic exponent $1/\nu$, skewness 1 and dispersion $(2C_1^{(1)})^{1/\nu}\gamma_{\mathrm{UWB}}\cos\left(\frac{\pi}{2\nu}\right)$. As a result, the characteristic function (CF) of A^2 conditioned on $C_1^{(1)}$ for $\nu > 1$ is given by

$$\psi_{A^2|C_1^{(1)}}(jv) = \exp\left[-(2C_1^{(1)})^{1/\nu}\gamma_{\mathrm{UWB}}\cos\left(\frac{\pi}{2\nu}\right)|jv|^{1/\nu}\left(1 - \frac{jv}{|jv|}\tan\left(\frac{\pi}{2\nu}\right)\right)\right]. \tag{23}$$

Using (23), we can rewrite (22) as

$$P_{\mathrm{e,TR}|C_1^{(1)},d_0=+1}^{(\mathrm{UWB})} \simeq \frac{1}{2} + \frac{1}{\pi}\int_0^\infty \left(\frac{1}{1+v^2}\right)^{q_\mathrm{TR}} \mathfrak{Re}\left\{\frac{\psi_{\mu_\mathrm{TR}}\left(\frac{-jv}{1+jv}\right)\psi_{A^2|C_1^{(1)}}\left(\frac{P^\mathrm{I}N_\mathrm{s}}{2WN_0}\frac{-jv}{1+jv}\right)}{jv}\right\} dv. \tag{24}$$

Similarly for $d_0 = -1$, the conditional BEP can be written as

$$P_{\mathrm{e,TR}|C_1^{(1)},d_0=-1}^{(\mathrm{UWB})} \simeq \frac{1}{2} + \frac{1}{\pi}\int_0^\infty \left(\frac{1}{1+v^2}\right)^{q_\mathrm{TR}} \times \mathfrak{Re}\left\{\frac{\psi_{\mu_\mathrm{TR}}\left(\frac{-jv}{1+jv}\right)\psi_{A^2|C_1^{(1)}}\left(\frac{P^\mathrm{I}N_\mathrm{s}}{2WN_0}\frac{jv}{1-jv}\right)}{jv}\right\} dv. \tag{25}$$

As discussed in [10], we can avoid averaging over $C_1^{(1)}$ in (24) and (25) by approximating the CF of A^2. Similar to [10], we approximate the expectation of (23) with respect to $C_1^{(1)}$ and obtain

$$\psi_{A^2}(jv) \simeq \left[1 + \Omega_\nu\gamma_{\mathrm{UWB}}\cos\left(\frac{\pi}{2\nu}\right)|jv|^{1/\nu} \times \left(1 - \frac{jv}{|jv|}\tan\left(\frac{\pi}{2\nu}\right)\right)\right]^{-k_\nu}. \tag{26}$$

Using (22) and (26), we have

$$P_{\mathrm{e,TR}|d_0=+1}^{(\mathrm{UWB})} \simeq \frac{1}{2} + \frac{1}{\pi}\int_0^\infty \left(\frac{1}{1+v^2}\right)^{q_\mathrm{TR}} \times \mathfrak{Re}\left\{\frac{\psi_{\mu_\mathrm{TR}}\left(\frac{-jv}{1+jv}\right)\psi_{A^2}\left(\frac{P^\mathrm{I}N_\mathrm{s}}{2WN_0}\frac{-jv}{1+jv}\right)}{jv}\right\} dv, \tag{27}$$

and for

$$P_{\mathrm{e,TR}|d_0=-1}^{(\mathrm{UWB})} \simeq \frac{1}{2} + \frac{1}{\pi}\int_0^\infty \left(\frac{1}{1+v^2}\right)^{q_\mathrm{TR}} \times \mathfrak{Re}\left\{\frac{\psi_{\mu_\mathrm{TR}}\left(\frac{-jv}{1+jv}\right)\psi_{A^2}\left(\frac{P^\mathrm{I}N_\mathrm{s}}{2WN_0}\frac{jv}{1-jv}\right)}{jv}\right\} dv. \tag{28}$$

As a result, the BEP of the AcR using TR signaling with BPAM in the presence of UWB Type 1 interference is given by

$$P_{\mathrm{e,TR}}^{(\mathrm{UWB})} = \frac{1}{2}\left(P_{\mathrm{e,TR},d_0=+1}^{(\mathrm{UWB})} + P_{\mathrm{e,TR},d_0=-1}^{(\mathrm{UWB})}\right). \tag{29}$$

B. Type 2 interference

With Type 2 interference, we still consider that the positions of the interferers and the shadowing terms do not change during the symbol but we remove all the other constraints of Type 1 interference. Due to the effect of the data modulation, of the hopping sequences and of the random amplitude sequences used by the interferers, the multipath components of each interferer signal change position and phase from one frame to another, even though the channel impulse response is constant over T_s. In the following, we consider the vector representing the aggregate interference over the entire symbol interval to be sub-Gaussian. As a result, we have $r_{1,j} \triangleq \zeta_{1,j,m} - \zeta_{2,j,m} \triangleq \sqrt{V}(G_{1,j,m} - G_{2,j,m})$ and $r_{2,j} \triangleq \zeta_{1,j,m} + \zeta_{2,j,m} = \sqrt{V}(G_{1,j,m} + G_{2,j,m})$. We can write the non-centrality parameters of $Y_{\mathrm{TR},1}$ and $Y_{\mathrm{TR},2}$ for $d_0 = +1$ as

$$\mu^{(\mathrm{UWB})}_{Y_{\mathrm{TR},1}} = \underbrace{\frac{E^{\mathrm{TR}}_\mathrm{s}}{N_0}\sum_{l=1}^{L_{\mathrm{CAP}}} h_l^2}_{\mu_{\mathrm{A,TR}}} + \underbrace{2\gamma^{\nu}_{\mathrm{UWB}}\frac{P^{\mathrm{I}}}{2WN_0}VC_1^{(2)}}_{\mu^{(\mathrm{UWB})}_{\mathrm{B,TR}}} + \underbrace{\sum_{j=0}^{\frac{N_\mathrm{s}}{2}-1}\sum_{m=0}^{2WT}\frac{1}{N_0}\frac{r_{1,j,m}w_{j,m}}{2W}}_{\mu^{(\mathrm{UWB})}_{\mathrm{C,TR}}}, \tag{30}$$

$$\mu^{(\mathrm{UWB})}_{Y_{\mathrm{TR},2}} = 2\gamma^{\nu}_{\mathrm{UWB}}\frac{P^{\mathrm{I}}}{2WN_0}VC_2^{(2)}, \tag{31}$$

where $C_1^{(2)} = \sum_{j=0}^{\frac{N_\mathrm{s}}{2}-1}\sum_{i=1}^{2WT}(G_{1,j,i} - G_{2,j,i})^2$ and $C_2^{(2)} = \sum_{j=0}^{\frac{N_\mathrm{s}}{2}-1}\sum_{i=1}^{2WT}(G_{1,j,i} + G_{2,j,i})^2$. Note that $C_1^{(2)}$ and $C_2^{(2)}$ are independent and follow a central chi-square distribution with $\frac{N_\mathrm{s}}{2}2WT$ degrees of freedom. Considering $\mu^{(\mathrm{UWB})}_{\mathrm{C,TR}}$ negligible [13], the approximate BEP conditioned on $C_1^{(2)}$ and $C_2^{(2)}$ can be expressed as

$$P^{(\mathrm{UWB})}_{\mathrm{e,TR}|C_1^{(2)},C_2^{(2)}} \simeq \frac{1}{2} + \frac{1}{\pi}\int_0^{\infty}\left(\frac{1}{1+v^2}\right)^{q_{\mathrm{TR}}} \times \Re\mathfrak{e}\left\{\frac{\psi_{\mu_{\mathrm{TR}}}\left(\frac{-jv}{1+jv}\right)\psi_V\left(g_{\mathrm{TR}|C_1^{(2)},C_2^{(2)}}(jv)2\gamma^{\nu}_{\mathrm{UWB}}\right)}{jv}\right\}dv, \tag{32}$$

where

$$g_{\mathrm{TR}|C_1^{(2)},C_2^{(2)}}(jv) = \frac{P_{\mathrm{I}}}{2WN_0}\left[C_1^{(2)}\frac{-jv}{1+jv} + C_2^{(2)}\frac{jv}{1-jv}\right], \tag{33}$$

and $\psi_V(jv)$ is the CF of the stable variable V. To obtain the BEP performance of AcR in the presence of UWB Type 2 interference, we simply need to numerically average (32) over $C_1^{(2)}$ and $C_2^{(2)}$.

V. Numerical results

In this section, we evaluate the performance of AcR in the presence of UWB MUI.[10] For the desired signal, we consider a bandpass UWB system with pulse duration $T_\mathrm{p} = 0.5$ ns, symbol interval $T_\mathrm{s} = 3200$ ns, and $N_\mathrm{s} = 32$. For simplicity, T_r is set such that there is no ISI or isi in the system, i.e., $T_\mathrm{f}^{\mathrm{TR}} = T_\mathrm{r}$ with $T_\mathrm{r} > T_\mathrm{g} - N_\mathrm{h}T_\mathrm{p}$. We consider a TH sequence of all ones ($c_j = 1$ for all j) and $N_\mathrm{h} = 2$. The desired signal is affected by a dense resolvable multipath channel, where each multipath amplitude is Nakagami distributed with fading severity index m and average power $\mathbb{E}\left\{h_l^2\right\}$, where $\mathbb{E}\left\{h_l^2\right\} = \mathbb{E}\left\{h_1^2\right\}\exp\left[-\epsilon(l-1)\right]$, for $l = 1,\dots,L$, are normalized such that $\sum_{l=1}^{L}\mathbb{E}\left\{h_l^2\right\} = 1$. For simplicity, the fading severity index m is assumed to be identical for all paths. The average power of the first arriving multipath component is given by $\mathbb{E}\left\{h_1^2\right\}$ and ϵ is the channel power decay factor. With this model, we denote the channel characteristic of the desired signal by (L,ϵ,m) for convenience. For the UWB interferers, they use the same waveform as the signal of interest with Nakagami fading channels and severity index m^{I} and average power $\mathbb{E}\left\{|h_l^{\mathrm{I}}|^2\right\}$. Like the desired UWB signals, we denote the channel characteristic of the interference signals by $(L^{\mathrm{I}},\epsilon^{\mathrm{I}},m^{\mathrm{I}})$.

[10]Note that all results shown are based on the approximate analytical method.

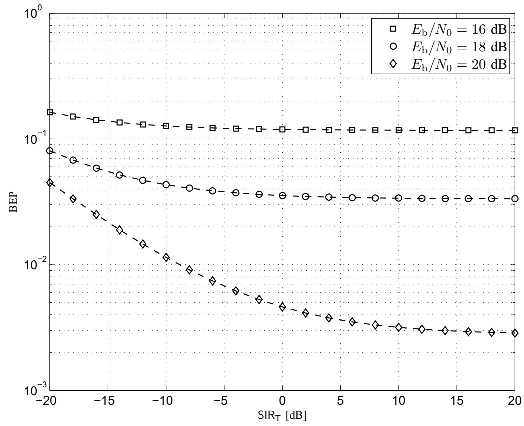

Fig. 1. BEP of AcR in the presence of Type 1 interference for $(L,\epsilon,m) = (32,0,3)$, $(L^{\mathrm{I}},\epsilon^{\mathrm{I}},m^{\mathrm{I}}) = (32,0,3)$, $T_\mathrm{f}^{\mathrm{I}} = 50$ ns, $\lambda = 0.01$, $\nu = 1.5$, and $\sigma_{\mathrm{I}} = 1.6$ dB.

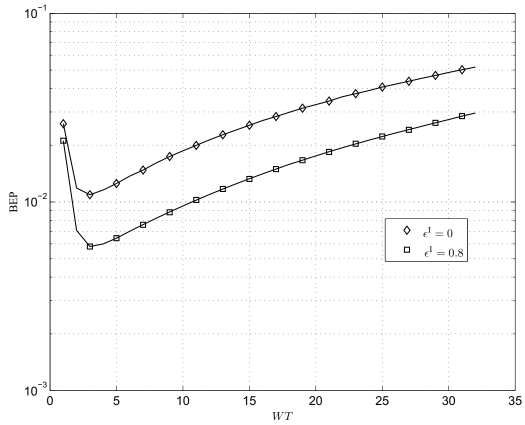

Fig. 2. BEP comparison of AcR in the presence of Type 1 interference as a function of WT for $E_\mathrm{b}/N_0 = 20$ dB, $\mathrm{SIR_T} = -20$ dB, $(L,\epsilon,m) = (32,0.4,3)$, $(L^{\mathrm{I}},\epsilon^{\mathrm{I}},m^{\mathrm{I}}) = (32,\epsilon^{\mathrm{I}},3)$, $T_\mathrm{f}^{\mathrm{I}} = 50$ ns, $\lambda = 0.01$, $\nu = 1.5$, and $\sigma_{\mathrm{I}} = 1.6$ dB.

A. BEP performance

1) Type 1 interference: Figure 1 compares the BEP performance of AcR in the presence of Type 1 interference with $(L,\epsilon,m) = (32,0,3)$ and $(L^{\mathrm{I}},\epsilon^{\mathrm{I}},m^{\mathrm{I}}) = (32,0,3)$. In Fig. 2, the BEP performance of AcR is plotted as a function of WT for $E_b/N_0 = 20$dB, $\mathrm{SIR_T} = -20$ dB, and $\lambda = 0.01$. It can be noticed that the interference channel PDP with

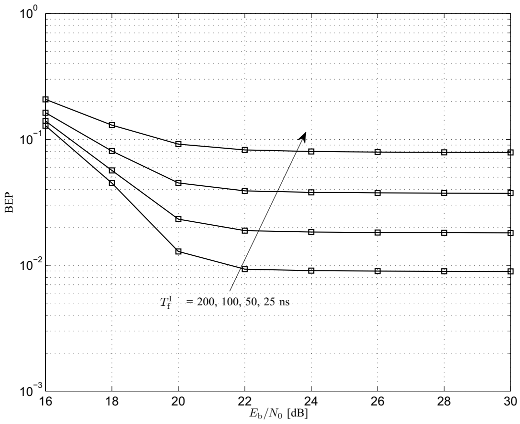

Fig. 3. Effect of pulse repetition interval T_f^I on the BEP performance of AcR in the presence of Type 1 interference for $E_b/N_0 = 20$ dB, $\mathsf{SIR_T} = -20$ dB, $(L, \epsilon, m) = (32, 0, 3)$, $(L^I, \epsilon^I, m^I) = (32, 0, 3)$, $\lambda = 0.01$, $\nu = 1.5$, and $\sigma_I = 1.6$ dB.

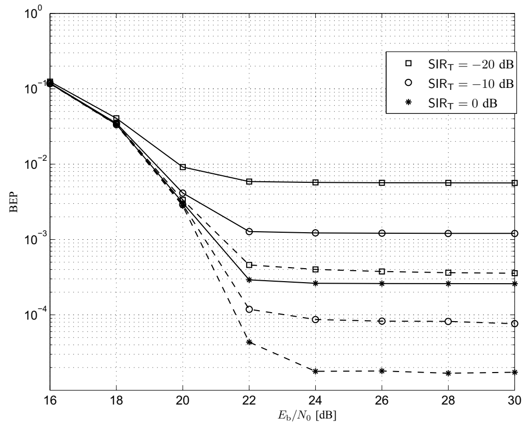

Fig. 4. Comparison of the effect of Type 1 interference (solid line) and Type 2 interference (dashed line) on the BEP performance of AcR for $(L, \epsilon, m) = (32, 0, 3)$, $(L^I, \epsilon^I, m^I) = (32, 0, 3)$, $T_f^I = 50$ ns, $\nu = 1.5$, $\sigma_I = 1.6$ dB.

a higher ϵ^I results in lesser performance degradation. This can be explained by the fact that with a steeper PDP, the interference signal energy is effectively concentrated in fewer multipath components and, thus leads to a lower probability of collision. In Fig. 3, the effect of pulse repetition T_f^I on the BEP performance of AcR is plotted, respectively. From these figures, we can clearly observe that better BEP performance is obtained for lower repetition rate due to lower probability of collision, given by T_g^I/T_f^I.

2) Type 2 interference: The numerical results below are obtained by averaging over many realizations of the variables $C_1^{(2)}$ and $C_2^{(2)}$. Lastly, in Fig. 4 the performance of AcR is compared for $(L, \epsilon, m) = (32, 0, 3)$, $(L^I, \epsilon^I, m^I) = (32, 0, 3)$, and $T_f^I = 50$ ns. From these figures, we see that the BEP performance is better for Type 2 interference compared to Type 1 interference. Furthermore, it is interesting to observe the trade-off between pulse repetition interval T_f^I and spatial density λ. From μ_{TR}, there is an equivalent relationship between T_f^I and λ. For example, when λ doubles, T_f^I should also double in order not to increase the effect of interference.

VI. Conclusions

In this paper, we investigated the effect of uncoordinated UWB network interference on the BEP performance of AcR. We first derived a statistical model of the aggregate interference based on multivariate stable distribution, which takes into consideration the spatial distribution of the interference nodes, the propagation characteristics of the interference signals, and the signaling parameters of the interference systems. Using our statistical UWB NWI model, we evaluated the BEP performance of AcR in different types of UWB NWI. Our proposed analytical framework allows a tractable BEP performance analysis and still provides valuable insight into the coexistence of UWB systems in wireless networks.

References

[1] M. Z. Win and R. A. Scholtz, "Ultra -wide bandwidth time -hopping spread-spectrum impulse radio for wireless multiple -access communications," *IEEE Trans. Commun.*, vol. 48, no. 4, pp. 679–691, Apr. 2000.

[2] T. Q. S. Quek and M. Z. Win, "Analysis of UWB transmitted-reference communication systems in dense multipath channels," *IEEE J. Sel. Areas Commun.*, vol. 23, no. 9, pp. 1863–1874, Sep. 2005.

[3] IEEE, "P802.15.4a/D7, approved draft amendment to IEEE standard for information technology-telecommunications and information exchange between systems-PART 15.4:wireless medium access control (MAC) and physical layer (PHY) specifications for low-rate wireless personal area networks (LR-WPANs): Amendment to add alternate PHY (amendment of IEEE std 802.15.4)," 2007.

[4] G. Durisi and G. Romano, "Simulation analysis and performance evaluation of an UWB system in indoor multipath channel," in *Proc. of IEEE Conf. on Ultra Wideband Systems and Techno.*, Baltimore, MD, Jun. 2002, pp. 255–258.

[5] B. Hu and N. Beaulieu, "Exact bit error rate analysis of TH-PPM UWB systems in the presence of multiple-access interference," *IEEE Commun. Lett.*, vol. 7, no. 12, pp. 572–574, Dec. 2003.

[6] Y. Dhibi and T. Kaiser, "On the impulsiveness of multiuser interferences in TH-PPM-UWB systems," *IEEE Trans. Signal Process.*, vol. 54, no. 7, pp. 2853–2857, Jul. 2006.

[7] E. Sousa, "Performance of a spread spectrum packet radio network link in a Poisson field of interferers," *IEEE Trans. Inf. Theory*, vol. 38, no. 6, pp. 1743–1754, Nov. 1992.

[8] J. Ilow, D. Hatzinakos, and A. Venetsanopoulos, "Performance of FH SS radio networks with interference modeled as a mixture of Gaussian and alpha-stable noise," *IEEE Trans. Commun.*, vol. 46, no. 4, pp. 509–520, Apr. 1998.

[9] P. C. Pinto, C.-C. Chong, A. Giorgetti, M. Chiani, and M. Z. Win, "Narrowband communication in a Poisson field of ultrawideband interferers," in *Proc. IEEE Int. Conf. on Ultra Wideband*, Waltham, MA, Sep. 2006, pp. 387–392.

[10] A. Rabbachin, T. Q. S. Quek, P. C. Pinto, I. Oppermann, and M. Z. Win, 'effect of aggregate narrowband interference on the UWB autocorrelation receiver," in *Proc. IEEE Int. Conf. on Ultra Wideband*, Hannover, GERMANY, Sep. 2008, pp. 79–83.

[11] D. Cassioli, M. Z. Win, and A. F. Molisch, "The ultra -wide bandwidth indoor channel: from statistical model to simulations," *IEEE J. Sel. Areas Commun.*, vol. 20, no. 6, pp. 1247–1257, Aug. 2002.

[12] J. Kingman, *Poisson Processes*, 1st ed. Oxford University Press, 1993.

[13] T. Q. S. Quek, M. Z. Win and D. Dardari, "Unified analysis of UWB transmitted-reference schemes in the presence of narrowband interference," *IEEE Trans. Wireless Commun.*, vol. 6, no. 6, pp. 2126–2139, Jun. 2007.

[14] J. Foerster, "Channel modeling sub-commitee report final," IEEE P802.15-02/490r1-SG3a, Mar. 2003.

[15] G. Samoradnitsky and M. S. Taqqu, *Stable Non-Gaussian Random Processes*, 1st ed. Chapman and Hall, 1994.